Interactive CardioVascular and Thoracic Surgery 24 (2017) 173–180
doi:10.1093/icvts/ivw284 Advance Access publication 28 September 2016

ORIGINAL ARTICLE

Cite this article as: Jahren SE, Winkler BM, Heinisch PP, Wirz J, Carrel T, Obrist D. Aortic root stiffness affects the kinematics of bioprosthetic aortic valves. Interact CardioVasc Thorac Surg 2017;24:173–80.

ADULT CARDIAC

Aortic root stiffness affects the kinematics of bioprosthetic aortic valves[†]

Silje Ekroll Jahren[a,*,†], Bernhard Michael Winkler[b,†], Paul Philipp Heinisch[b], Jessica Wirz[a], Thierry Carrel[b] and Dominik Obrist[a]

[a] ARTORG Center, University of Bern, Bern, Switzerland
[b] Department of Cardiovascular Surgery, University Hospital Bern, Bern, Switzerland

* Corresponding author. University of Bern, ARTORG Center, Murtenstrasse 50, 3008 Bern, Switzerland. Tel: +41-31-6327587; fax: +41-31-6327576; e-mail: silje.jahren@artorg.unibe.ch (S.E. Jahren).

Received 5 April 2016; received in revised form 2 June 2016; accepted 20 July 2016

Abstract

OBJECTIVES: In this study, the influence of aortic root distensibility on the haemodynamic parameters and valve kinematics of a bioprosthetic aortic valve was investigated in a controlled *in vitro* experiment.

METHODS: An Edwards INTUITY Elite 21 mm sutureless aortic valve (Edwards Lifesciences, Irvine, CA, USA) was inserted in three transparent aortic root phantoms with different wall thicknesses (0.55, 0.85 and 1.50 mm) mimicking different physiological distensibilities. Haemodynamic measurements were performed in an *in vitro* flow loop at heart rates of 60, 80 and 100 bpm with corresponding cardiac outputs of 3.5, 4.0 and 5.0 l/min and aortic pressures of 100/60, 120/90 and 145/110 mmHg, respectively. Aortic valve kinematics were assessed using a high-speed camera. The geometric orifice area (GOA) was measured by counting pixels in the lumen of the open aortic valve. The effective orifice area (EOA) was calculated from the root-mean-square value of the systolic aortic valve flow rate and the mean systolic trans-valvular pressure gradient.

RESULTS: The tested aortic root phantoms reproduce physiological distensibilities of healthy individuals in age groups ranging from 40 to 70 years (±10 years). The haemodynamic results show only minor differences between the aortic root phantoms: the trans-valvular pressure gradient tends to increase for stiffer aortic roots, whereas the systolic aortic valve flow rate remains constant. As a consequence, the EOA decreased slightly for less distensible aortic roots. The GOA and the aortic valve opening and closing velocities increase significantly with reduced distensibility for all haemodynamic measurements. The resulting mean systolic flow velocity in the aortic valve orifice is lower for the stiffer aortic root.

CONCLUSIONS: Aortic root distensibility may influence GOA and aortic valve kinematics, which affects the mechanical load on the aortic valve cusps. Whether these changes have a significant effect on the onset of structural valve deterioration of bioprosthetic heart valves needs to be further investigated.

Keywords: Bioprosthetic valve • Aortic valve • Aortic root distensibility

INTRODUCTION

The native aortic valve shows competent function without early structural failure for challenging physiological demands. The aortic root including the sinus portions has long been known to be important for the correct functioning of the aortic valve cusps and therefore also for the competence of the aortic valve [1–3]. During systole, vortices form in the sinus portions and affect the position of the cusps. It has been suggested that they contribute during end-systole to the prevention of jet formation and competent closure of the valve [4, 5]. In 1999, a study by Yacoub *et al.* [6] indicated the importance of further studies of the haemodynamic influence of the aortic root on aortic valve performance.

The distensibility of the aortic root is related to the opening and closing kinematics of the native aortic valve and to an increase of the valve orifice area during exercise [7]. These physiological mechanisms may be altered in stiff roots, e.g. heavily calcified roots. The distensibility of the aortic root also has an effect on the blood flow patterns in the aortic root and on the related mechanical stresses, which may affect aortic valve cusp tissue remodelling or pathological changes [3]. Degeneration and subsequent calcification of the aortic valve have been connected to zones with high mechanical stress [8]. Valvular diseases such as aortic stenosis are

[†] Presented at the Swiss Cardio Annual Meeting, Lausanne, Switzerland, 15–17 June 2016.
[†] The first two authors contributed equally to this study.

associated with aortic valve tissue and annulus thickening, reduction in elasticity and the ability to adapt to changes during the cardiac cycle, reduction in distensibility, and increasing stiffness of the aortic valve cusps and root [8, 9]. In patients with bicuspid aortic valves, the reduction in aortic wall elasticity was associated with aneurysms of the ascending aorta, left ventricular (LV) hypertrophy and aortic valve regurgitation [10]. In humans older than 50–60 years of age, it has been reported that decreased distensibility and changes in the aortic root geometry can lead to different biomechanical and haemodynamic characteristics of the aortic valve [8, 11].

In the light of the general trend towards bioprosthetic and transcatheter aortic valves, the topic of aortic root distensibility is of growing interest because bioprosthetic structural valve deterioration (SVD) and anatomical changes are important prognostic factors. The ideal design of artificial heart valves has not been identified [12]. Serious problems remain with respect to the long-term performance of bioprosthetic valves and patient outcomes [13–16] related to SVD, thrombosis, tissue overgrowth, paravalvular leaks and calcification. Different independent factors have been suggested to influence SVD [8]. In recent studies [17, 18], the sinus portions and the distensibility of aortic root grafts have been shown to affect aortic valve kinematics after aortic valve sparing procedures. The objective of this study is to investigate the effect of aortic root distensibility in the context of bioprosthetic aortic valves. For this purpose, we studied haemodynamic parameters and kinematics of a bioprosthetic aortic valve in a controlled *in vitro* experiment with systematically varied aortic root distensibilities.

MATERIALS AND METHODS

Aortic root phantoms

Transparent aortic root phantoms of three different wall thicknesses (0.55, 0.85 and 1.5 mm) were manufactured using ELASTOSIL® RT 601 A/B silicone (Wacker Silicones, Wacker Chemistry AG, Munich, Germany) in a 9:1 ratio (by weight) to mimic three different aortic root distensibilities. The aortic root phantoms were manufactured by applying the silicone in layers to a 3D-printed negative model of a standard aortic root geometric configuration with a diameter of 2.1 cm [19]. Polymerization of each silicone layer was done during 3D rotation for an equal distribution of the silicone. The aortic annulus and inflow tract were stabilized with a strip of compression bandage immersed in the silicone. An Edwards INTUITY Elite 21 mm sutureless aortic valve (Edwards Lifesciences, Irvine, CA, USA) was inserted in the aortic root phantoms, and the aortic valve stent was dilated with a balloon three times at 4.5, 4.5 and 5.0 atm, respectively, to avoid paravalvular leakage. The aortic valve was secured with a surgical thread tied around the aortic root phantoms at the annulus to avoid valve migration (Fig. 1A).

Left heart simulator

The aortic root phantoms with the inserted aortic valve were tested in a left heart simulator (Fig. 1) described previously [20]. The left heart simulator consisted of four polymethylmethacrylate chambers representing the left atrium (LA) and the left ventricle (LV), a water-filled chamber enclosing the aortic root phantom to allow undistorted optical access and a chamber representing the systemic arterial tree compliance. A bileaflet mechanical valve separated the LA and LV chambers, mimicking the mitral valve (MV), and a gated valve between the compliance chamber and the LA chamber representing the systemic resistance. A mixture of 40/60% glycerine and water at room temperature was used to mimic the viscosity of blood.

Haemodynamic measurements

Haemodynamic measurements for each aortic root phantom were performed for three different haemodynamic configurations:

(i) At 60 bpm, with a cardiac output of ∼3.5 l/min and an aortic pressure of 100/60 mmHg.
(ii) At 80 bpm, with a cardiac output of ∼4.0 l/min and an aortic pressure of 120/90 mmHg.
(iii) At 100 bpm, with a cardiac output of ∼5.0 l/min and an aortic pressure of 145/110 mmHg.

For the first haemodynamic configuration, the settings for the compliance chamber, the gated valve (peripheral resistance) and the pump stroke volume were adjusted to obtain the values for the respective parameters (aortic pressure and cardiac output) at 60 bpm. For the second and third configurations, the settings for the compliance chamber and the gated valve remained the same and only the pump stroke volume and the heart rate were adjusted to achieve the respective parameters. For all haemodynamic measurements, these settings remained the same for each configuration and between each aortic root phantom.

The LV and aortic pressures (measured in the LV and the compliance chamber, respectively), the pump flow and the MV flow were recorded. All haemodynamic measurements were performed for 25 s with a sampling rate of 200 Hz.

Aortic valve kinematics assessment

A high-speed camera (Basler piA640-210gc GigE, Basler AG, Ahrensburg, Germany) captured the aortic valve movements during the haemodynamic measurements described above at a frame rate of 200 Hz for 20 s. The camera was mounted either sideways to visualize cusp motion in the axial plane of the aortic root phantoms as well as the dilatation of the phantom walls (Fig. 1A) or axially (retrograde axial view) to visualize the cusp motion in the valvular plane (Fig. 1B). Experiments for each haemodynamic configuration were performed twice with the camera in either the sideways or axial position, yielding a total of six performed measurements for each aortic root phantom. The haemodynamic measurements and the camera frames were synchronized using a synthetic trigger signal.

Data analysis

The measured data were post-processed using MATLAB (The MathWorks, Natick, MA, USA). Some heartbeats were excluded from the analysis (on average 2 ± 1 heartbeats per measurement) because of some missing camera frames. Haemodynamic parameters and aortic valve kinematic parameters were calculated for each heartbeat for all measurements. Data from at least 15

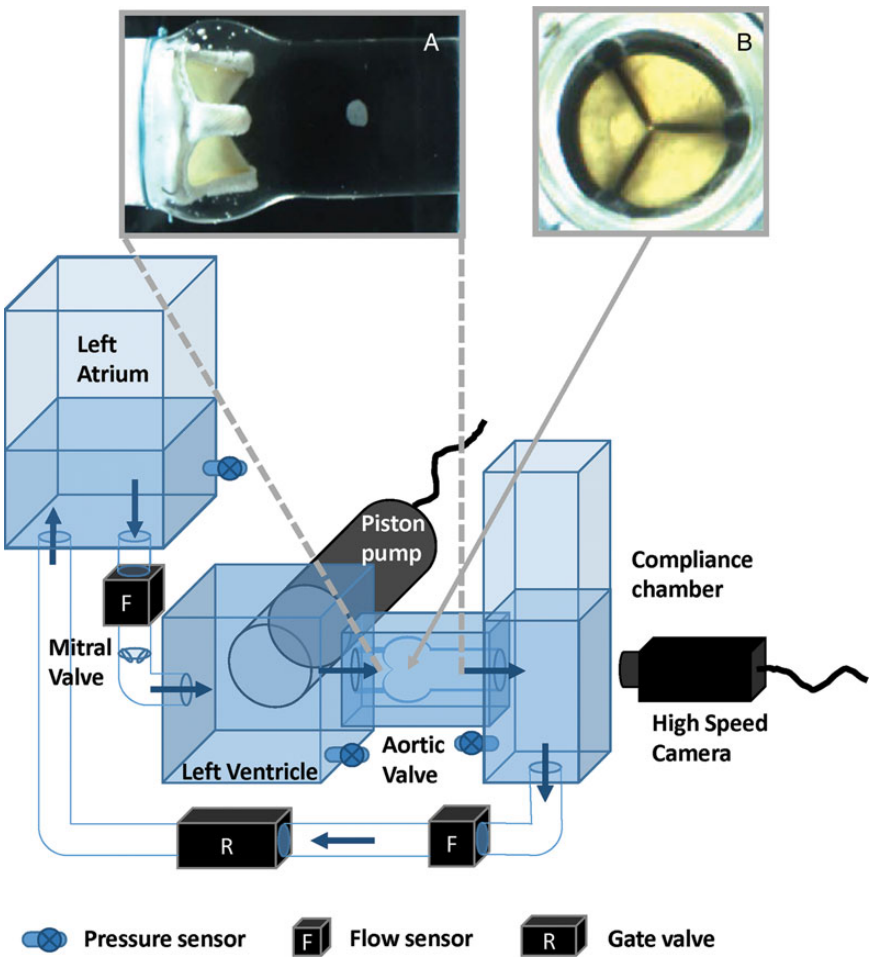

Figure 1: Overview of the left heart simulator set-up [20]. (**A**) Sideway camera view of the aortic root phantom with the aortic valve; (**B**) retrograde axial camera view of the aortic valve.

heartbeats were used to obtain ensemble-averaged heartbeats, mean values and standard deviations of these parameters. The aortic valve flow was calculated as the measured pump flow minus the measured MV flow. Effective orifice area (EOA) was calculated as [21]:

$$\mathrm{EOA} = \frac{Q_{\mathrm{RMS}}}{51.6 \cdot \sqrt{dP_{\mathrm{mean}}}} \ (\mathrm{cm}^2) \qquad (1)$$

where Q_{RMS} (ml/s) is the root-mean-square value of systolic flow through the aortic valve and dP_{mean} (mmHg) is the mean systolic trans-valvular pressure gradient.

The camera frames taken in the axial view were used to measure the geometric orifice area (GOA) by counting (frame by frame) the pixels in the lumen of the open aortic valve, which was identified by an edge detection algorithm using MATLAB. The conversion from pixels to centimetres was calibrated using the distance (~100 pixels) between two well-defined reference points on the stent ring. The uncertainty in the reference length measurement was ±2 pixels, which led to an uncertainty of ±4% in the resulting area measurements. The robustness of the method for measuring the GOA was tested by comparing the results obtained with slight variations of the method (e.g. different parameter settings for the edge detection method, different choice of reference points for calibration). It was found that the results were robust and accurate within the given range of uncertainty.

The rate of change of GOA ($\Delta\mathrm{GOA}/\Delta t$) was calculated using MATLAB to assess the opening and closing velocities of the aortic valve. The mean systolic flow velocity in the aortic valve orifice was calculated as $Q_{\mathrm{RMS}}/\mathrm{GOA}$ (m/s). The diameter of the aortic root phantoms was determined with respect to the width of the ascending aorta of the aortic root phantoms from the frames taken in a sideways position. The aortic root phantom distensibility was calculated as [22]

$$\begin{aligned}\mathrm{Distensibility} &= 100\frac{A - A_0}{A_0(P - P_0)} \\ &= 100\frac{D^2 - D_0^2}{D_0^2(P - P_0)} \ (\%/\mathrm{mmHg}) \end{aligned} \qquad (2)$$

where A (cm^2) is the systolic ascending aortic lumen area at the systolic aortic pressure P (mmHg) and A_0 (cm^2) is the diastolic ascending aortic lumen area at the diastolic aortic pressure P_0 (mmHg). Accordingly, D (cm) is the systolic ascending aortic lumen diameter at the systolic aortic pressure P (mmHg) and D_0 (cm) is the diastolic ascending aortic lumen diameter at the diastolic aortic pressure P_0 (mmHg).

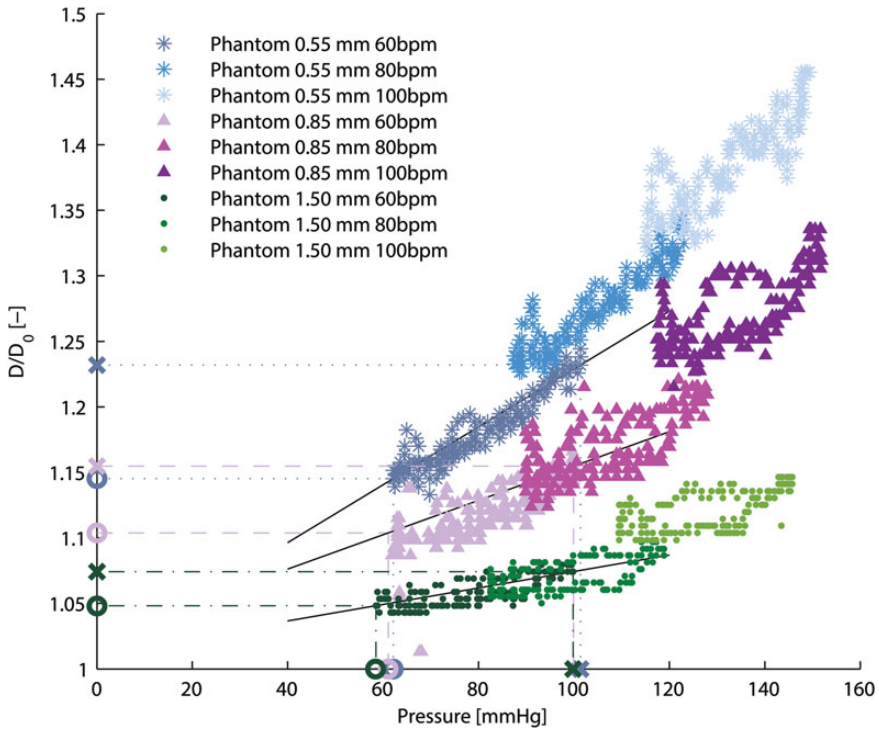

Figure 2: Relative aortic root phantom diameter (D/D_0) at the ascending aorta as a function of aortic pressure for all aortic root phantoms and haemodynamic measurements. The values used to calculate the aortic root phantom distensibilities are marked on the axis with *X* for the systolic values and *O* for the diastolic values. The solid black lines indicate the slopes between the corresponding systolic and diastolic values.

Table 1: Overview of mean haemodynamic parameters for all measurements

Phantom thickness (mm)	HR (bpm)	Aortic systolic pressure (mmHg)	Aortic diastolic pressure (mmHg)	Mean pressure gradient (mmHg)	Mean systolic aortic valve rms flow (ml/s)	Cardiac flow output (l/min)	Camera position
0.55	59.8 (0.3)	101.8 (0.2)	62.2 (0.2)	9.8 (0.2)	264.0 (1.7)	3.5 (0.03)	Sideways
	59.9 (0.2)	102.2 (0.4)	63.8 (0.3)	9.9 (0.2)	266.6 (2.2)	3.5 (0.03)	Axial
	78.6 (0.2)	123.4 (0.2)	87.6 (0.4)	11.3 (0.2)	294.5 (2.6)	4.2 (0.03)	Sideways
	78.6 (0.3)	123.4 (0.2)	86.8 (0.2)	11.4 (0.3)	296.1 (2.2)	4.2 (0.03)	Axial
	94.7 (2.8)	145.5 (2.8)	110.6 (3.3)	12.6 (0.4)	315.8 (5.0)	4.7 (0.09)	Sideways
	98.3 (0.5)	148.7 (0.4)	113.9 (0.4)	12.3 (0.3)	319.9 (3.7)	4.7 (0.04)	Axial
0.85	56.5 (0.2)	101.2 (0.7)	62.3 (0.6)	9.6 (0.2)	248.0 (2.9)	3.5 (0.03)	Sideways
	58.4 (0.2)	105.7 (0.3)	65.1 (0.4)	9.6 (0.1)	261.7 (1.9)	3.6 (0.03)	Axial
	78.5 (0.3)	128.2 (0.2)	89.8 (0.2)	12.3 (0.2)	287.3 (3.4)	4.3 (0.03)	Sideways
	78.1(0.3)	128.3 (0.7)	91.0 (0.8)	12.1 (0.3)	291.0 (3.0)	4.4 (0.04)	Axial
	97.3 (0.5)	153.9 (0.7)	118.2 (0.4)	12.9 (0.3)	313.4 (4.9)	5.0 (0.03)	Sideways
	95.3 (0.3)	150.3 (0.4)	115.6 (0.2)	13.5 (0.3)	305.5 (3.9)	5.0 (0.03)	Axial
1.50	56.0 (0.3)	100.1 (0.2)	58.4 (0.2)	8.5 (0.2)	264.7 (2.3)	3.6 (0.03)	Sideways
	58.5 (0.3)	101.3 (0.4)	60.1 (0.3)	10.0 (0.1)	267.8 (1.5)	3.7 (0.03)	Axial
	78.1 (0.3)	119.5 (0.3)	81.9 (0.1)	12.2 (0.3)	297.8 (3.3)	4.4 (0.03)	Sideways
	78.2 (0.4)	121.5 (0.2)	82.7 (0.3)	12.4 (0.2)	302.0 (2.6)	4.4 (0.03)	Axial
	94.7 (1.0)	145.5 (0.8)	108.3 (1.2)	14.9 (0.4)	327.4 (3.3)	5.1 (0.05)	Sideways
	98.3 (0.4)	146.3 (0.3)	110.1 (0.5)	14.6 (0.4)	321.7 (3.7)	5.1 (0.05)	Axial

The standard deviation is given in parentheses.
HR: heart rate; rms: root-mean-square.

Analysis of variance (ANOVA) was performed to test if there was a statistically significant difference between the means of the averaged systolic GOAs of the different aortic root phantoms, as well as between the means of the EOAs and the aortic valve opening and closing velocities. The ANOVA was performed separately for each haemodynamic configuration. Pairwise *t*-tests were performed to determine between which aortic root phantoms these parameters were significantly different. The differences were considered significant for *P*-values less than 0.05.

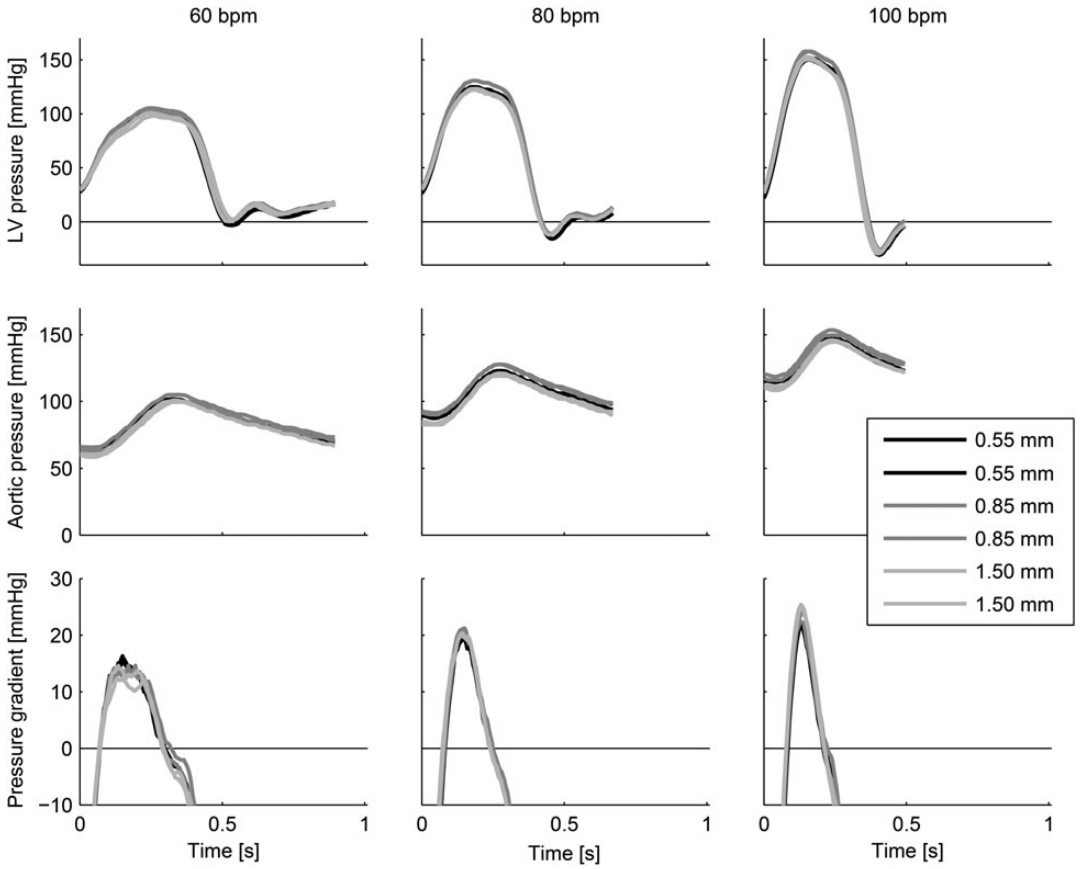

Figure 3: Aortic and left ventricular pressures and trans-valvular pressure gradients for all measurements showing the ensemble-averaged heartbeats.

RESULTS

Aortic root phantom distensibility

Figure 2 shows the relative diameter (D/D_0) of the aortic root phantoms at different aortic pressures during a heartbeat for $D_0 = 2.1$ cm. The diameter increases with increasing aortic pressure and shows hysteretic behaviour. The resulting distensibilities were found to be 0.53, 0.30 and 0.13%/mmHg, according to equation (2), for a systolic-to-diastolic aortic pressure of ∼100/60 mmHg for the aortic root phantom with wall thickness 0.55, 0.85 and 1.50 mm, respectively. The distensibility of the aortic root adds to the systemic compliance (Windkessel effect) provided by the large compliance chamber (Fig. 1). However, a comparison of the systolic volumes stored in the aortic root versus the volume changes in the compliance chamber shows that the contribution of the aortic root is negligible.

Haemodynamic results

The haemodynamic results for the different aortic root phantoms are listed in Table 1. The trans-valvular pressure gradient dP_{mean} was similar for the measurements at 60 bpm, whereas it tended to be larger for lower aortic root distensibilities at 80 and 100 bpm. Figure 3 shows the measured pressures in the aorta, the LV and the trans-valvular pressure gradient for all measurements. Clearly, the different aortic root phantoms did not significantly affect these haemodynamic parameters.

Aortic valve kinematics

Figure 4 shows the GOA plotted over time for the ensemble-averaged heartbeat at 100 bpm for the three different aortic root phantoms and the rate of change in GOA, indicating the aortic valve opening and closing velocity. The GOA increased with decreasing distensibility of the aortic root phantom, and the aortic valve opening and closing velocities were higher. For further illustration of the results, a video sequence (Video 1) of the valve kinematics is provided.

Figure 5 shows the mean aortic valve opening and closing velocities for all haemodynamic configurations. The velocities increased with decreasing distensibility for all heartbeats. This effect was more significant for higher heart rates and higher aortic pressures and flow. The aortic valve opening and closing velocities were significantly different between all aortic root phantoms at 100 bpm ($P < 0.005$ between all aortic root phantoms), as well as between the 0.55 and 1.50 mm thick phantoms for the haemodynamic measurements performed at 60 and 80 bpm ($P = 0.01$, $P < 0.005$, respectively). Additionally, the increase in both aortic valve opening and closing velocities was significant between the 0.85 mm and the 1.50 mm phantoms at 80 bpm ($P = 0.01$, $P = 0.01$, respectively) and for the aortic valve opening velocity between the 0.55 mm and the 0.85 mm phantom at 80 bpm ($P < 0.005$).

Figure 6 shows the GOA, the EOA and the mean systolic flow velocity (Q_{RMS}/GOA) in the aortic valve orifice for all measurements. EOA and mean systolic flow velocity tended to decrease with decreasing distensibility, whereas the GOA increased. The increase in GOA with decreasing distensibility was significant between all aortic

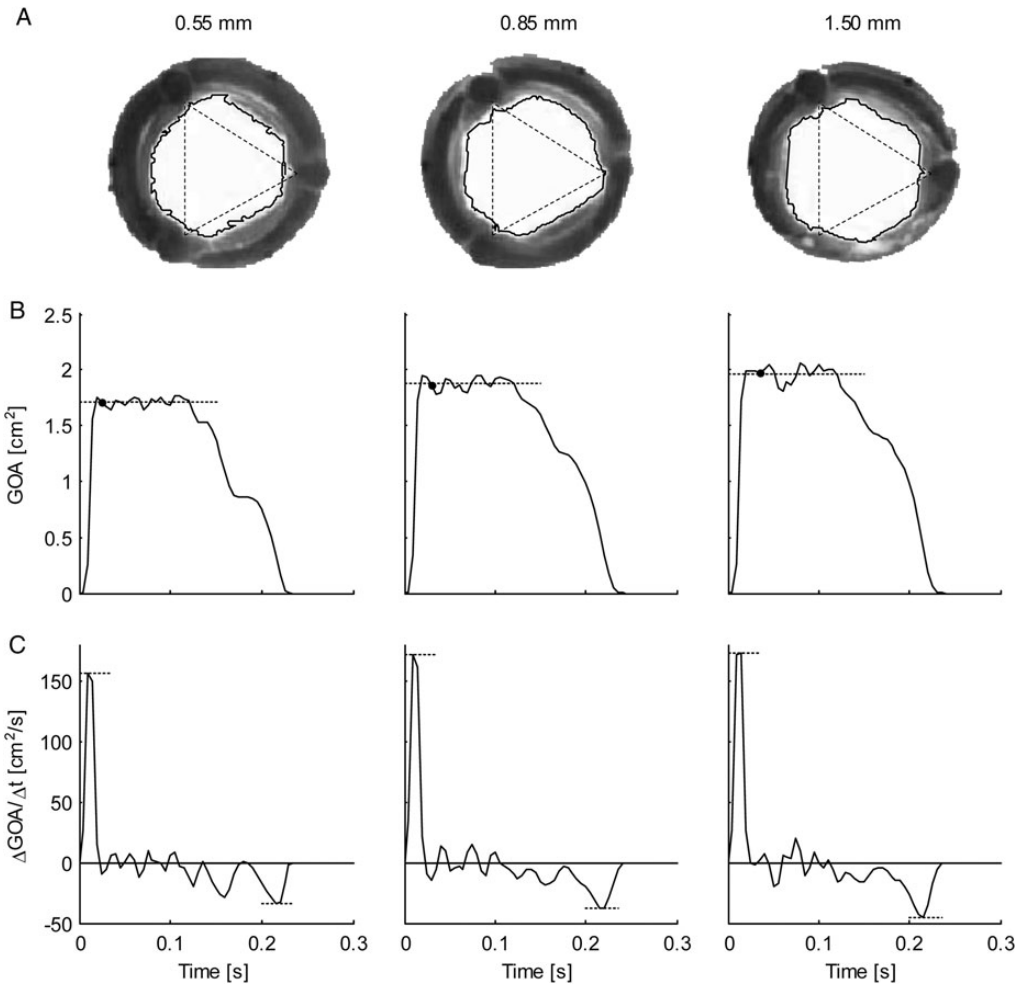

Figure 4: (**A**) Representative frames (retrograde axial camera view) taken of the aortic valve during systole for the three aortic root phantoms (from left to right: 0.55, 0.85 and 1.50 mm wall thickness) at 100 bpm. The solid lines show the borders of the geometric orifice area (GOA); the corners of the triangles (dotted lines, equal size) indicate the locations of the valve commissures. (**B**) Ensemble-averaged GOA plotted over time. The dotted lines indicate the mean mid-systolic GOA, and the black dots indicate the timing of the frames in (**A**). (**C**) Ensemble-averaged rate of change in GOA per time unit ($\Delta GOA/\Delta t$). The dotted lines indicate the maximum and minimum rates of change (aortic valve opening and closing velocities, respectively).

root phantoms for all haemodynamic states ($P < 0.005$ between all phantoms). The decrease in EOA with decreasing distensibility was significant for all aortic root phantoms for the haemodynamic measurements at 80 and 100 bpm ($P < 0.005$ between all phantoms), whereas it was insignificant for any of the phantoms for the haemodynamic measurements at 60 bpm (ANOVA: $P = 0.79$).

DISCUSSION

The aim of this study was to investigate the effect of aortic root distensibility on the haemodynamic parameters and valve kinematics of a sutureless bioprosthetic aortic valve. The measured distensibilities of the aortic root phantoms were found to be in the physiological range reported for healthy individuals [22]. The distensibility of the aortic root phantom with 0.55 mm wall thickness corresponded to values found for healthy individuals in the age group 40 ± 10 years; the phantom with lowest distensibility (1.50 mm wall thickness) corresponded to the age group 70 ± 10 years for healthy individuals. The stiffest phantom may also be a good model for younger patients with cardiovascular diseases that may impact the stiffness of the aortic root (e.g. calcifications).

The haemodynamic performance of the Edwards INTUITY Elite 21 mm aortic valve was found to be in accordance with values given in the literature [23, 24], indicating that the left heart simulator reproduces appropriate physiological flow conditions in the aortic valve and the aortic root. The haemodynamic results showed only minor variations between the different aortic root phantoms. This finding implies that aortic root distensibility has no significant effect on the overall haemodynamic performance of a bioprosthetic aortic valve.

Aortic root distensibility affected the GOA and the aortic valve opening and closing velocities significantly (Fig. 5). We found that the aortic valve opened more (higher GOA) for stiffer aortic root phantoms. This phenomenon was more pronounced for higher heart rates. Most significantly, the GOA for 100 bpm was almost 20% larger for the least distensible aortic root than for the most distensible root. At the same time, the systolic trans-valvular pressure gradients dP_{mean} tended to increase for less distensible roots and, consequently, the EOA decreased slightly. This result can be attributed to the smaller systolic lumen of the less distensible aortic root phantom, which led to higher viscous pressure losses (see Fig. 2: ascending aortic diameter for 100 bpm at peak systole for the thick-walled phantom was ∼20% smaller than for the thin-walled phantom).

Video 1: Video sequence with axial and side views of the bioprosthetic aortic valve inserted in the three different aortic root phantoms (from left to right: 0.55, 0.85 and 1.50 mm wall thickness) at 100 bpm and 5 l/min cardiac output. In the first part of the video, four heartbeats are shown in real time (200 frames/s). The second part shows two heartbeats in slow motion (10 frames/s).

The reason why the aortic valve opened more in a stiff aortic root is not well understood. We suspect that it is related to the flow conditions in the sinus portions, which may depend on the distension of the sinus portion. Most likely, the vortices that formed in the sinus portions of the stiff aortic roots had a different character from the vortices in the soft roots, which offered a larger volume for vortex formation. More detailed investigations of the flow in the sinus portions are required to understand the complex dynamics of the aortic root and to explain the increase of GOA in stiffer roots.

The increased GOA in stiffer aortic roots led to a lower mean systolic flow velocity (Q_{RMS}/GOA) in the aortic valve orifice. This result implies that the systolic wall-shear-stress acting on the aortic valve cusps was probably lower for these roots. It also suggests that the Reynolds number of the systolic blood stream was lower, which is expected to lead to lower levels of turbulence in the aortic root. At the same time, the stiffer aortic root phantoms showed higher aortic valve opening and closing velocities, which might lead to higher mechanical load on the aortic valve cusps during opening and closure.

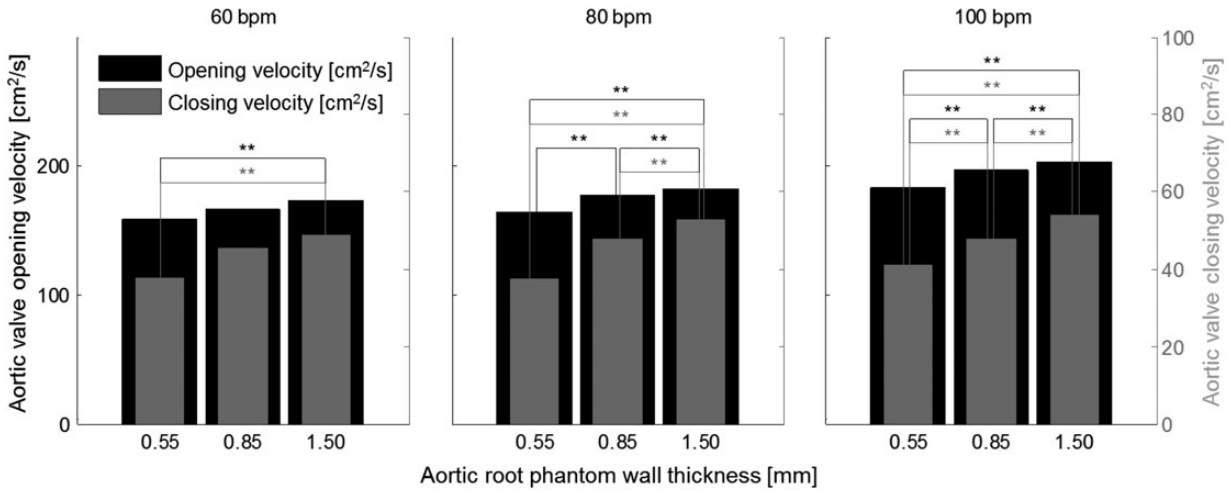

Figure 5: Mean aortic valve opening (black) and closing (grey) velocities for all measurements. **Significantly different aortic valve opening (black) or closing (grey) velocities.

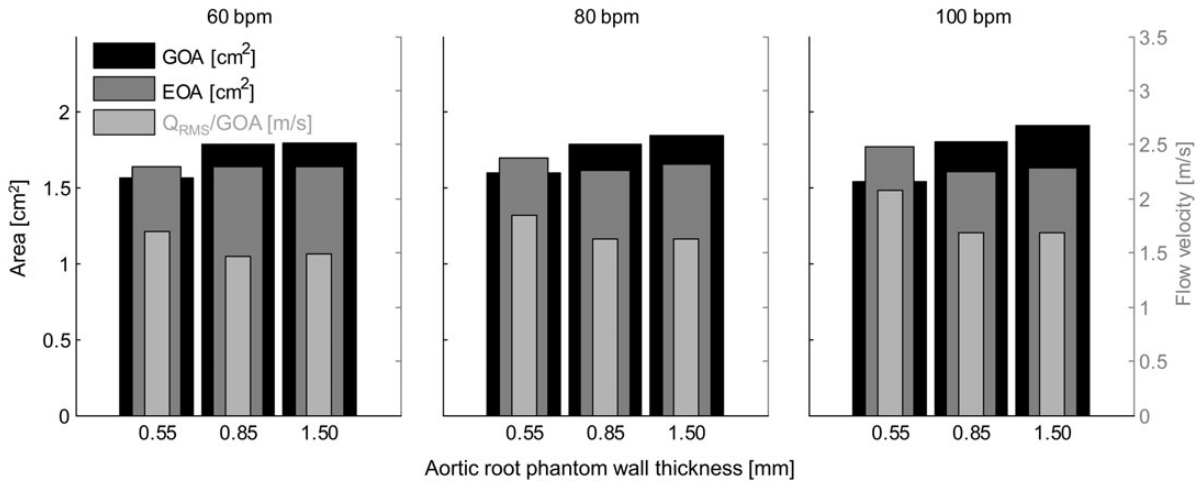

Figure 6: The mean values of the geometric orifice area (GOA), the effective orifice area (EOA) and the mean systolic flow velocity through the aortic valve orifice for all measurements.

One limitation of this study is that only one type of bioprosthetic aortic valve was tested. The Edwards INTUITY Elite sutureless aortic valve is a stented surgical valve similar to the well-studied Edwards PERIMOUNT Magna valve when it comes to cusp design [24, 25]. It is expected that other stented bioprosthetic valves with similar cusp designs will exhibit the same effects related to aortic root stiffness. However, for different bioprosthetic aortic valve design concepts, e.g. stentless or transcatheter designs, the effect of aortic root distensibility can be different and needs further investigation. A second limitation is that only one aortic valve size and aortic root size were tested. The distensibility of the aortic root also depends on the chosen prosthetic valve size and type [26]. Aortic valve size versus aortic root size is expected to influence the flow field behind the valve and thereby also the aortic valve kinematics. Similarly, aortic root morphology and aortic valve positioning in the annulus are expected to have an influence. In this study, only one position of the aortic valve and only one aortic root morphological type were investigated.

Additional research is necessary to clarify the changes in distensibility in the long-term. In particular, scar tissue formation after surgical valve replacement may influence aortic root distensibility [26]. With a better understanding of aortic root physiology, future research on aortic valve replacement should take into account the integrated structural and functional asymmetry of aortic root dynamics to minimize stress on the aortic cusps to mitigate premature SVD.

In conclusion, we have shown that the GOA increases for less distensible aortic roots, and with it also the aortic valve opening and closing velocities. The larger GOA is expected to decrease the systolic wall-shear-stress, acting on the aortic valve cusps due to the lower mean flow velocity and to reduce turbulence levels in the aortic root. The higher opening and closing speeds of the aortic valve lead to higher mechanical load on the cusps for stiffer aortic roots. Aortic root stiffness might influence the onset of SVD, due to the alteration in GOA, cusp kinematics and wall-shear-stress. Whether or not these factors have a significant influence on the lifetime of the bioprosthetic valve needs further investigation.

FUNDING

This work was supported through basic research funds of the University of Bern.

Conflict of interest: none declared.

REFERENCES

[1] Cheng A, Dagum P, Miller DC. Aortic root dynamics and surgery: from craft to science. Philos Trans R Soc Lond B Biol Sci 2007;362:1407–19.
[2] Robicsek F. Leonardo da Vinci and the sinuses of Valsalva. Ann Thorac Surg 1991;52:328–35.
[3] Butcher JT, Simmons CA, Warnock JN. Mechanobiology of the aortic heart valve. J Heart Valve Dis 2008;17:62–73.
[4] Bellhouse BJ, Reid KG. Fluid mechanics of the aortic valve. J Fluid Mech 1969;35:721–35.
[5] Bellhouse BJ, Bellhouse FH. Mechanism of closure of the aortic valve. Nature 1968;217:86–7.
[6] Yacoub MH, Kilner PJ, Birks EJ, Misfeld M. The aortic outflow and root: a tale of dynamism and crosstalk. Ann Thorac Surg 1999;68:S37–43.
[7] Sripathi VC, Tech B, Kumar RK, Balakrishnan KR. Further insights into normal aortic valve function : role of a compliant aortic root on leaflet opening and valve orifice area. Ann Thorac Surg 2004;77:844–51.
[8] Singh R, Strom JA, Ondrovic L, Joseph B, VanAuker MD. Age-related changes in the aortic valve affect leaflet stress distributions: implications for aortic valve degeneration. J Heart Valve Dis 2008;17:290–9.
[9] Barbetseas J, Alexopoulos N, Brili S, Aggeli C, Marinakis N, Vlachopoulos C *et al*. Changes in aortic root function after valve replacement in patients with aortic stenosis. Int J Cardiol 2006;110:74–9.
[10] Grotenhuis HB, Ottenkamp J, Westenberg JJM, Bax JJ, Kroft LJM, de Roos A. Reduced aortic elasticity and dilatation are associated with aortic regurgitation and left ventricular hypertrophy in nonstenotic bicuspid aortic valve patients. J Am Coll Cardiol 2007;49:1660–5.
[11] Gavrilenkov VI, Iukhnev AD, Maslevtsov DV. Vozrastnaia dinamika biomekhanicheskikh i gidrodinamicheskikh svoistv klapanno-aortal'nogo kompleksa cheloveka [Age-dependent dynamics of biomechanical and hydrodynamic properties of the valve-aortic complex of man (In Russian)]. Vestn Khir Im I Grek 2000;159:20–5.
[12] Yoganathan AP, He Z, Casey Jones S. Fluid mechanics of heart valves. Annu Rev Biomed Eng 2004;6:331–62.
[13] Bre LP, McCarthy R, Wang W. Prevention of bioprosthetic heart valve calcification: strategies and outcomes. Curr Med Chem 2014;21:2553–64.
[14] Starr A, Fessler CL, Grunkemeier G, He G-W. Heart valve replacement surgery: past, present and future. Clin Exp Pharmacol Physiol 2002;29:735–8.
[15] Hammermeister K, Sethi GK, Henderson WG, Grover FL, Oprian C, Rahimtoola SH. Outcomes 15 years after valve replacement with a mechanical versus a bioprosthetic valve: final report of the Veterans Affairs randomized trial. J Am Coll Cardiol 2000;36:1152–8.
[16] Weber A, Noureddine H, Englberger L, Dick F, Gahl B, Aymard T *et al*. Ten-year comparison of pericardial tissue valves versus mechanical prostheses for aortic valve replacement in patients younger than 60 years of age. J Thorac Cardiovasc Surg 2012;144:1075–83.
[17] De Paulis R, Salica A, Pisani G, Morbiducci U, Weltert L, Maselli D. Hemodynamics of the aortic valve and root: implications for surgery. Ann Cardiothorac Surg 2013;2:40–3.
[18] Salica A, Pisani G, Morbiducci U, Scaffa R, Massai D, Audenino A *et al*. The combined role of sinuses of Valsalva and flow pulsatility improves energy loss of the aortic valve. Eur J Cardio-Thoracic Surg 2016;49:1222–7.
[19] Swanson WM, Clark RE. Dimensions and geometric relationships of the human aortic value as a function of pressure. Circ Res 1974;35:871–82.
[20] Jahren SE, Heinisch PP, Wirz J, Winkler BM, Carrel T, Obrist D. Hemodynamic performance of Edwards intuity valve in a compliant aortic root model. 2015 37th Annual International Conference of IEEE Engineering in Medicine and Biology Society (EMBC) 2015;3315–8.
[21] Saikrishnan N, Kumar G, Sawaya FJ, Lerakis S, Yoganathan AP. Accurate assessment of aortic stenosis: a review of diagnostic modalities and hemodynamics. Circulation 2014;129:244–53.
[22] Redheuil A, Yu WC, Wu CO, Mousseaux E, De Cesare A, Yan R *et al*. Reduced ascending aortic strain and distensibility: earliest manifestations of vascular aging in humans. Hypertension 2010;55:319–26.
[23] Kocher AA, Laufer G, Haverich A, Shrestha M, Walther T, Misfeld M *et al*. One-year outcomes of the surgical treatment of aortic stenosis with a next generation surgical aortic valve (TRITON) trial: a prospective multicenter study of rapid-deployment aortic valve replacement with the EDWARDS INTUITY valve system. J Thorac Cardiovasc Surg 2013;145:110–6.
[24] Borger MA, Dohmen P, Misfeld M, Mohr FW. Current trends in aortic valve replacement: development of the rapid deployment EDWARDS INTUITY valve system. Expert Rev Med Devices 2013;10:461–70.
[25] Borger MA, Nette AF, Maganti M, Feindel CM. Carpentier-edwards perimount magna valve versus medtronic hancock II: a matched hemodynamic comparison. Ann Thorac Surg 2007;83:2054–8.
[26] Funder JA, Ringgaard S, Frost MW, Wierup P, Klaaborg K-E, Hjortdal V *et al*. Aortic root distensibility and cross-sectional areas in stented and subcoronary stentless bioprostheses in pigs. Interact CardioVasc Thorac Surg 2010;10:976–80.